Synthesis and Structure of the Polymetallic Yttrium Alkoxide Complex $Y_3(\mu_3\text{-}OCMe_3)(\mu_3\text{-}Cl)(\mu\text{-}OCMe_3)_3(OCMe_3)_4(THF)_2$ and Related Complexes: $Ln_3(\mu_3\text{-}OR)(\mu_3\text{-}X)(\mu\text{-}OR)_3$ Building Blocks in Yttrium and Lanthanide Alkoxide Chemistry[1]

William J. Evans,* Mark S. Sollberger, and Timothy P. Hanusa

Contribution from the Department of Chemistry, University of California, Irvine, Irvine, California 92717. *Received May 26, 1987*

Abstract: YCl_3 reacted with 3 equiv of $NaOCMe_3$ in THF to form $Y_3(\mu_3\text{-}OCMe_3)(\mu_3\text{-}Cl)(\mu\text{-}OCMe_3)_3(OCMe_3)_4(THF)_2$ (**1**) in 80% yield. Complex **1** crystallized from toluene in the orthorhombic space group *Pmcn* with unit cell dimensions a = 16.976 (6) Å, b = 13.466 (5) Å, c = 25.823 (8) Å, and Z = 4 for D_{calcd} = 1.265 g cm^{-3}. Least-squares refinement on the basis of 1654 observed reflections led to a final R value of 0.064. The complex contains a trigonal-planar arrangement of yttrium atoms with μ-$OCMe_3$ groups along the edges of the Y_3 triangle, a μ_3-$OCMe_3$ ligand on one side of the plane, and a μ_3-Cl on the other. Two terminal $OCMe_3$ ligands are attached to one yttrium atom and each of the other yttrium atoms are ligated by a terminal $OCMe_3$ group and a THF of solvation. YCl_3 reacted with 3 equiv of $NaOCMe_3$ in THF in the presence of Me_3COH to form **2**, which has been characterized as an isomer of **1** by spectroscopic and analytical methods. Complex **1** can be isomerized to **2** by heating in THF in the presence of Me_3COH. Recrystallization of **2** from hexane gives crystals that have a hexagonal unit cell with a = 17.648 (11) Å and c = 11.171 (4) Å. YCl_3 reacted with 2 equiv of $LiOCMe_3$ in THF to give a complex product mixture. Extraction with and recrystallization from hexane gave crystals of $[Y_4(\mu_3\text{-}OCMe_3)_2(\mu\text{-}OCMe_3)_4(OCMe_3)_4(\mu_4\text{-}O)(\mu\text{-}Cl)_2Li_4(\mu\text{-}OCMe_3)_2]_2$ (**3**). **3** crystallized in the space group $C2/c$ with unit cell dimensions a = 24.920 (6) Å, b = 14.012 (5) Å, c = 41.548 (12) Å, β = 88.40 (2)°, and Z = 8 for D_{calcd} = 1.234 g cm^{-3}. Least-squares refinement on the basis of 3743 observed reflections led to a final R value of 0.11. Complex **3** contains two Y_4 units that have a butterfly arrangement of yttrium atoms with μ_3-$OCMe_3$ groups over each wing, μ-$OCMe_3$ groups along the edges of the wings, and a μ_4-O ligand located centrally within bonding distance of all four yttrium atoms. Each yttrium atom is attached to one terminal $OCMe_3$ group. The wing-tip yttrium atoms are also attached to chloride ligands which link the two Y_4 units via $Li(OR)_2$ bridging moieties. $LaCl_3$ reacted with 3 equiv of $NaOCMe_3$ in THF to give **4**, which, on the basis of spectroscopic and analytical data, is similar to **1** and **2** except that both triply bridging positions are occupied by $OCMe_3$ groups, i.e., $La_3(\mu_3\text{-}OCMe_3)_2(\mu\text{-}OCMe_3)_3(OCMe_3)_4(THF)_2$. Recrystallization of **4** from toluene gave crystals with an orthorhombic unit cell with a = 20.543 (11) Å, b = 17.477 (9) Å, and c = 17.905 (7) Å.

The organometallic chemistry of yttrium and the lanthanide metals currently is undergoing rapid development and a rich and diverse chemistry is being discovered.[2-8] Most investigations have involved complexes containing cyclopentadienyl and substituted cyclopentadienyl groups as co-ligands. The $C_5R_5^-$ ligands (R = H, CH_3) are ideal for yttrium and the lanthanide complexes since they satisfy the electrostatic and steric requirements of these large electropositive metal ions.[2] The $C_5R_5^-$ groups also provide stability and solubility to complexes containing more reactive functionalities such as alkyl and hydride ligands thereby allowing Ln-R and Ln-H chemistry to be elaborated.

Although the $C_5R_5^-$ groups are ideal co-ligands for the initial investigations of the chemistry of yttrium and lanthanide alkyls and hydrides, cyclopentadienyl groups have some limitations when practical exploitation of this reactivity is considered. Their sensitivity to protonic reagents and oxygen in these complexes precludes many types of reactions and reaction conditions. In some cases, their steric bulk can inhibit reactivity. For example, the C_5H_5 groups sterically block the reactivity of the hydride ligands in the trimetallic $\{[(C_5H_5)_2Ln(\mu\text{-}H)]_3(\mu_3\text{-}H)\}^-$ ions (Ln = Y, Er, Lu)[9,10] severely limiting the reactivity of these tetrahydride complexes.[11]

As part of a general program to make oxygen-stabilized organoyttrium and organolanthanide complexes,[12] we have begun to study the utility of alkoxide groups as co-ligands alternative to $C_5R_5^-$ groups. Alkoxide ligands, RO^-, are attractive due to the strength of the Y-O bond and because the R group can be extensively varied to control the solubility and steric saturation of the complex.

Alkoxide complexes of yttrium and the lanthanides have been known for many years.[13,14] The first lanthanide metal alkoxide, $La(OMe)_3$, was prepared by Bradley and Faktor in 1958.[15] Since then, $Ln(OR)_3$ complexes have been reported for Ln = La, Pr, Nd, Sm, Gd, Tb, Dy, Ho, Er, Yb, Lu, and Y.[16-27] The general

(1) Reported in part at the 191st National Meeting of the American Chemical Society, New York, NY, April 1986, INOR 291, and the 2nd International Conference on the Chemistry and Technology of Lanthanides and Actinides, Lisbon, Portugal, April 1987, P(I)19.

(2) Evans, W. J. *Adv. Organomet. Chem.* **1985**, *24*, 131-177 and references therein.

(3) Evans, W. J. *Polyhedron* **1987**, *6*, 803-805 and references therein.

(4) Watson, P. L.; Parshall, G. W. *Acc. Chem. Res.* **1985**, *18*, 51-56 and references therein.

(5) Schumann, H.; Genthe, W. In *Handbook on the Physics and Chemistry of Rare Earths*; Gschneidner, K. A., Jr., Eyring, L., Eds.; Elsevier: Amsterdam, 1985; Vol. 7, Chapter 53 and references therein.

(6) Marks, T. J.; Ernst, R. D. In *Comprehensive Organometallic Chemistry*; Wilkinson, G., Stone, F. G. A., Abel, E. W., Eds.; Pergamon: 1982; Chapter 21.

(7) Forsberg, J. H.; Moeller, T. In *Gmelin Handbook of Inorganic Chemistry 8th Ed. Sc, Y, La-Lu Part D6*; Moeller, T., Kruerke, U., Schleitzer-Rust, E., Eds.; Springer-Verlag: Berlin, 1983; pp 137-282 and references therein.

(8) Kagan, H. B.; Namy, J. L. In *Handbook on the Physics and Chemistry of Rare Earths*; Gschneidner, K. A., Jr., Eyring, L., Eds.; Elsevier: Amsterdam, 1984; Vol. 6, Chapter 50.

(9) Evans, W. J.; Meadows, J. H.; Wayda, A. L.; Hunter, W. E.; Atwood, J. L. *J. Am. Chem. Soc.* **1982**, *104*, 2015-2017.

(10) Evans, W. J.; Meadows, J. H.; Hanusa, T. P. *J. Am. Chem. Soc.* **1984**, *106*, 4454-4460.

(11) Evans, W. J.; Sollberger, M. S.; Khan, S. I.; Bau, R. *J. Am. Chem. Soc.*, in press.

(12) Evans, W. J.; Sollberger, M. S. *J. Am. Chem. Soc.* **1986**, *108*, 6095-6096.

(13) Bradley, D. C.; Mehrotra, R. C.; Gauer, D. P. *Metal Alkoxides*; Academic: London, 1978.

(14) Mehrotra, R. C.; Kapoor, P. N.; Batwara, J. M. *Coord. Chem. Rev.* **1980**, *31*, 67-91.

(15) Bradley, D. C.; Faktor, M. M. *Chem. Ind. (London)* **1958**, 1332.

(16) Misra, S. N.; Misra, T. N.; Kapoor, R. N.; Mehrotra, R. C. *Chem. Ind. (London)* **1963**, 120.

(17) Misra, S. N.; Misra, T. N.; Mehrotra, R. C. *Aust. J. Chem.* **1968**, *21*, 797-800.

(18) Brown, L. M.; Mazdiyasni, K. S. *Inorg. Chem.* **1970**, *9*, 2783-2786.

0002-7863/88/1510-1841$01.50/0

Table I. NMR Data for Complexes 1, 2, and 4

^{1}H NMR

complex	solvent	μ_3-OCMe$_3$	μ-OCMe$_3$	OCMe$_3$	THF
1	THF-d_8[a,b]	1.88 (s, 9 H)	1.50 (s, 18 H)	1.31 (s, 18 H), 1.24 (s, 9 H)	
			1.43 (9 H)	1.22 (s, 9 H)	
2	THF-d_8[b]	1.71 (s, 9 H)	1.48 (s, 18 H)	1.31 (s, 18 H), 1.25 (s, 9 H)	
			1.41 (s, 9 H)	1.18 (s, 9 H)	
	toluene-d_8[a]				
	(25 °C)[c]	1.88 (br)	1.68 (br)	1.49 (br), 1.47 (br)	2.09 (m), 1.35 (m)
	(0 °C)	1.91 (s, 9 H)	1.71 (s, 18 H)	1.52 (s, 18 H), 1.50 (s, 9 H)	2.09 (m)
			1.68 (s, 9 H)	1.47 (s, 9 H)	1.35 (m)
	pyridine-d_5[a]	2.02 (s, 9 H)	1.57 (s, 9 H)	1.53 (s, 18 H), 1.50 (s, 9 H)	3.63 (m, 8 H)
			1.56 (s, 18 H)	1.36 (s, 9 H)	1.59 (m, 8 H)
4	THF-d_8[b]	1.72 (s, 18 H)	1.51 (s, 18 H)	1.23 (br s, 36 H)	
			1.45 (s, 9 H)		
	pyridine-d_5	1.97 (s, 18 H)	1.66 (s, 18 H)	1.40 (br s, 36 H)	3.63 (m, 8 H)
			1.56 (s[c])		1.59 (m[c])

^{13}C NMR

complex	solvent	OCMe$_3$	OC(CH_3)$_3$	THF
1	THF-d_8[d]	76.9, 74.1, 74.1	36.3, 36.2, 36.1	69.4
		72.8, 72.2, 72.2	36.0, 35.3	27.6
2	THF-d_8	74.4, 72.9, 72.9	36.9, 36.5, 36.4	69.4
		72.2, 71.8, 71.8	36.0, 35.8	27.6
4	THF-d_8	73.5, 73.3, 72.5	36.8, 36.6, 36.3	69.4
		72.4	36.1	27.6
	pyridine-d_5[d]	72.0, 71.8, 70.9	35.5, 35.5, 35.0	67.9
		70.8	34.9	25.9
	benzene-d_6[c,d]	not observed	35.9, 35.5	71.1
				25.6

[a] In THF-d_8, toluene-d_8, pyridine-d_5 referenced to residual H at δ 1.79, 1.81, and 8.71, respectively. [b] Coordinated THF is seen as a broad singlet at approximately 0.45 ppm upfield from the solvent peaks. [c] Overlapping peaks. [d] In THF-d_8, pyridine-d_5, benzene-d_6 referenced to C at δ 68.6, 150.0, 128.7, respectively.

methods used for the preparation of lanthanide alkoxides are shown below in eq 1–4.[13-27]

$$2Ln + 6ROH \xrightarrow{HgCl_2} 2Ln(OR)_3 + 3H_2 \quad (1)$$

$$LnCl_3 + 3ROH + 3NH_3 \rightarrow Ln(OR)_3 + 3NH_4Cl \quad (2)$$

$$LnCl_3 + 3MOR \xrightarrow{ROH} Ln(OR)_3 + 3MCl \quad M = Li, Na, or K \quad (3)$$

$$LnCl_3 \cdot xROH + 3MOR \xrightarrow{ROH} Ln(OR)_3 + 3MCl \quad (4)$$

For R = alkyl in eq 1–4, no X-ray crystallographic studies have confirmed the simple monomeric structure implied by the reported formulas.[21] The literature contains conflicting results regarding the degree of oligomerization of these species. Some reports present evidence for discrete monomeric Ln(OR)$_3$ species,[16,17] while others describe oligomeric products.[14,22,25] In addition, repeated reports of chloride contamination,[14,17,24,25] alkali metal contamination,[25] and the presence of dehydrogenation byproducts[14,25] make the simplicity implied in these reactions subject to serious question. The best example of this has been the reaction of $NdCl_3$ with $NaOCHMe_2$, following reaction 4, which resulted in the hexametallic cluster $Nd_6(OCHMe_2)_{17}Cl$ with no evidence of a simple trisalkoxide species.[19]

Table II. IR Data for Complexes 1, 2, and 4 (cm^{-1})

1	2	4	NaOCMe$_3$
2960 (vs, br)	2940 (vs, br)	2940 (vs, br)	2960 (vs, br)
1465 (m)	1470 (m)	1470 (m)	1470 (m)
1380 (m)	1380 (m)		1380 (m)
1360 (s)	1360 (m)	1360 (s)	1360 (s)
1200 (vs, br)	1210 (vs, br)	1210 (vs, br)	1210 (vs, br)
1015 (sh)	1030 (sh)	1030 (m)	1030 (m)
1000 (s)	1000 (s)	980 (s)	
930 (s)	950 (s)	935 (s)	930 (m)
920 (sh)	920 (m)	910 (s)	
870 (vw)	880 (w)	880 (sh)	
760 (w)	770 (m)	760 (m)	
		730 (w)	720 (w)

Since steric factors are so important in the chemistry of yttrium and the lanthanide elements,[2,3] we felt it was essential to obtain more structural data on the alkoxide complexes we would use as starting materials for C_5R_5 free organoyttrium and organolanthanide systems. In this report we describe the synthesis and structural features of yttrium and lanthanum alkoxide complexes which represent prototypical starting materials for synthesis of organoyttrium and organolanthanide alkoxide alkyl and hydride complexes. We have chosen Y and La because these metals are representative of late[28] and early lanthanide chemistry, respectively, and provide diamagnetic compounds characterizable by NMR spectroscopy. To keep the spectroscopy as simple as possible we have worked exclusively with the *tert*-butoxide ligand which gives soluble complexes with a single ^{1}H NMR resonance per ligand.

Experimental Section

All of the complexes described below are extremely air- and moisture-sensitive. Therefore, both the syntheses and subsequent manipulations of these compounds were conducted with rigorous exclusion of air and water with use of Schlenk, vacuum line, and glovebox (Vacuum/

(19) Andersen, R. A.; Templeton, D. H.; Zalkin, A. *Inorg. Chem.* **1978**, *17*, 1962–1965.
(20) Sankhla, S.; Misra, S. N.; Kapoor, R. N. *Chem. Ind. (London)* **1965**, 382–383.
(21) Hitchcock, P. B.; Lappert, M. F.; Singh, A. *J. Chem. Soc., Chem. Commun.* **1983**, 1499–1501. Recently the structure of a monomeric aryloxide complex has been reported: Hitchcock, P. B.; Lappert, M. F.; Smith, R. G. *Inorg. Chim. Acta* **1987**, *139*, 183–184.
(22) Sankhla, B. S.; Kapoor, R. N. *Can. J. Chem.* **1966**, *44*, 2131–2137. Sankhla, B. S.; Kapoor, R. N. *Aust. J. Chem.* **1967**, *20*, 2013–2016.
(23) Batwara, J. M.; Tripathi, U. D.; Mehrotra, R. K.; Mehrotra, R. C. *Chem. Ind. (London)* **1966**, 1379.
(24) Mehrotra, R. C.; Batwara, J. M. *Inorg. Chem.* **1970**, *9*, 2505–2510.
(25) Mazdiyasni, K. S.; Lynch, C. T.; Smith, J. S. *Inorg. Chem.* **1966**, 342–346.
(26) Mehrotra, A.; Mehrotra, R. C. *Indian J. Chem.* **1972**, *10*, 532–535.
(27) Tripathi, U. D.; Batwara, J. M.; Mehrotra, R. C. *J. Chem. Soc. (A)* **1967**, 991–992.
(28) Evans, W. J.; Hanusa, T. P.; Meadows, J. H.; Hunter, W. E.; Atwood, J. L. *Organometallics* **1987**, *6*, 295–301 and references therein.

Atmospheres HE-83 Dri-Lab) techniques. *tert*-Butyl alcohol was dried over and distilled from CaH_2. $NaOCMe_3$ was prepared from sodium in *tert*-butyl alcohol at 25 °C. Removal of the excess *tert*-butyl alcohol by rotary evaporation at 60–80 °C left a partially solvated material $NaOCMe_3 \cdot xMe_3COH$, $x = 0.33$–0.50 (by elemental analysis). Sublimation at 150 °C and 10^{-4} Torr gave the completely desolvated $NaOCMe_3$. $NaOCMe_3$ dissolves in THF to give a completely colorless clear solution. In the presence of solvated *tert*-butyl alcohol, a cloudy solution is observed. Physical measurements and purification of the other reagents have been described previously.[29]

$Y_3(\mu_3\text{-}OCMe_3)(\mu_3\text{-}Cl)(\mu\text{-}OCMe_3)_3(OCMe_3)_4(THF)_2$ (1). In the glovebox, $NaOCMe_3$ (277 mg, 2.88 mmol) was dissolved in 6 mL of THF and added by pipet to a flask containing a stirred suspension of YCl_3 (188 mg, 0.96 mmol) in 8 mL of THF. After being stirred overnight the reaction mixture was transferred to a centrifuge tube and centrifuged. The solution was decanted away from a pasty insoluble residue which was analyzed for yttrium content (5%) and discarded. The solvent was removed from the solution by rotary evaporation leaving a colorless hexane soluble product, **1** (268 mg, 80%). X-ray quality crystals of **1** were grown from a concentrated solution in toluene at 29 °C. Anal. Calcd for $Y_3C_{40}H_{88}O_{10}Cl$: Y, 25.86. Found: Y, 25.2. NMR and IR data are given in Tables I and II.

$Y_3(\mu_3\text{-}OCMe_3)(\mu_3\text{-}Cl)(\mu\text{-}OCMe_3)_3(OCMe_3)_4(THF)_2$ (2). In the glovebox, $NaOCMe_3 \cdot {}^1/_3Me_3COH$ (0.437 g, 3.6 mmol) in 8 mL of THF was added by pipet to a flask containing YCl_3 (0.221 g, 1.13 mmol) stirring in 8 mL of THF. After being stirred for 2 h at 29 °C the reaction mixture was centrifuged and the solution was decanted, leaving behind a pasty residue. Removal of the solvent from the solution by rotary evaporation left a colorless crystalline product, **2** (0.283 g, 73%). Anal. Calcd for $Y_3C_{40}H_{88}O_{10}Cl$: Y, 25.86. Found: Y, 26.1. Isopiestic molecular weight,[30] Calcd: 1031. Found: 1085.

$[Y_4(\mu_3\text{-}OCMe_3)_2(\mu\text{-}OCMe_3)_4(OCMe_3)_4(\mu_4\text{-}O)(\mu\text{-}Cl)_2Li_4(\mu\text{-}OCMe_3)_2]_2$ (3). In the glovebox, $LiOCMe_3$ (0.867 g, 11 mmol) in 12 mL of THF was added by pipet to a flask containing YCl_3 (1.057 g, 5.4 mmol) stirring in 10 mL of THF. The reactants were stirred 3 days at 29 °C. The reaction mixture was centrifuged and the solution decanted, leaving behind a pasty solid. Removal of solvent from the solution by rotary evaporation left an oily residue. The residue was extracted with toluene, the mixture was centrifuged, and the solution was decanted. Removal of the solvent from the solution by rotary evaporation left an oily residue that was extracted with hexane. The solvent was removed from the solution leaving a colorless solid. The crystalline product **3** was isolated in low yield from a concentrated solution of this material in hexane. The crystals, once isolated, were insoluble even in THF.

$La_3(\mu_3\text{-}OCMe_3)_2(\mu\text{-}OCMe_3)_3(OCMe_3)_4(THF)_2$ (4). In the glovebox, $NaOCMe_3$ (294 mg, 3.06 mmol) was dissolved in 10 mL of THF and added by pipet to a flask containing a stirred suspension of $LaCl_3$ (250 mg, 1.02 mmol). After being stirred for 3 days the reaction mixture was centrifuged and the solution was decanted leaving behind a pasty residue that was analyzed for lanthanum content (6%) and discarded. The solvent was removed from the solution by rotary evaporation leaving the colorless product **4** (361 mg, 87%). X-ray quality crystals were grown from a concentrated solution in toluene at −20 °C. Anal. Calcd for $La_3C_{44}H_{97}O_{11}$: La, 34.19. Found: La, 32.0.

X-ray Crystallography. $Y_3(\mu_3\text{-}OCMe_3)(\mu_3\text{-}Cl)(\mu\text{-}OCMe_3)_3(OCMe_3)_4(THF)_2$ (1). General procedures for data collection and reduction have been described previously.[31,32] A crystal measuring 0.27 × 0.27 × 0.55 mm was sealed under N_2 in a glass capillary and mounted on a Syntex $P2_1$ diffractometer. Lattice parameters were determined at 25 °C from the angular settings of 15 computer-centered reflections with $9° \le 2\theta \le 20°$. Relevant crystal and data collection parameters for the present study are given in Table III. During the data collection, the intensities of three standard reflections measured every 100 reflections decreased by 15%; a correction for decay was later applied. The data were corrected for absorption. Systematic absences established the space group as either $Pn2_1a$ or $Pmcn$ (nonstandard settings of $Pna2_1$ and $Pnma$). Statistics favored the centrosymmetric $Pmcn$ and this choice was fully supported at all stages of the structure solution and refinement. Direct methods (MULTAN 80)[33] were used to locate the metal atoms and difference Fourier techniques provided the positions of the remaining non-hydrogen atoms. Atoms Y(2), Cl, O(1), C(1), C(3), O(3), C(8), C(9), O(4), C(11), C(13), O(5), C(14), C(16), and C(25)–C(30) lie on a crystallographic mirror plane. Some disorder was apparent in the terminal $OCMe_3$ group containing O(4) and C(11)–C(13). This was treated with use of a two-site model involving a 180° rotation between the *tert*-butyl groups. Refinement of the partial occupancies led to a 1:1 ratio for these sites. C(13A) and C(13B), which lie on the mirror plane, were subsequently fixed at 0.25 occupancy, and C(12A) and C(12B) were fixed at 0.50 occupancy. Difference maps revealed the presence of a six-membered ring, lying on the mirror plane, which on the basis of spectroscopic and analytical data was identified as a toluene molecule. A final difference map revealed a peak of intensity 0.82 e $Å^{-3}$ at a distance of 1.02 Å from C(25), one of the atoms of this ring. This may be due to the missing methyl group on the toluene ring, although it failed to refine properly as a carbon atom. There were no other recognizable features. The ring was refined with isotropic thermal parameters. Final fractional coordinates and selected bond length and angle data are given in Tables IV, V, and VI, respectively, and in the supplementary material.

Table III. Crystal Data and Summary of Intensity Data Collection and Structure Refinement for **1** and **3**

compound	**1**	**3**
formula	$Y_3C_{40}H_{88}O_{10}Cl(C_7H_9)$	$Y_4C_{40}H_{90}O_{11}Cl_2(Li_4C_8H_{18}O_2)$
mol wt	1124.448	1347.667
space group	*Pmcn*	*C2/c*
cell constants		
a (Å)	16.976 (6)	24.920 (6)
b (Å)	13.466 (5)	14.012 (5)
c (Å)	25.823 (8)	41.548 (12)
β (deg)		88.40 (2)
cell volume ($Å^3$)	5903 (4)	14501 (8)
molecules/unit cell	4	8
D(calcd) (g cm^{-3})	1.265	1.234
temp (K)	298	298
μ(calcd) (cm^{-1})	30.34	33.13
radiation	Mo Kα, λ = 0.71073 Å	Mo Kα, λ = 0.71073 Å
tranmsn factor range (min–max)	0.695–0.764	0.58–0.87
max crystal dimens (mm)	0.27 × 0.27 × 0.55	0.32 × 0.18 × 0.22
scan width in 2θ		
from Kα_1 (deg)	−1.2	−1.0
from Kα_2 (deg)	+1.2	+1.0
scan rate (deg min^{-1})	1.5–12	3.0–12
bkgd counting	estimated from 96-step peak profile	estimated from 96-step peak profile
std. reflns	223, 400, 406	004, 11-1, 313
decay of stds (%)	15	0
2θ range	4–45	4–45
total unique reflns	4046	9544
unique data with $I \ge 3\sigma(I)$	1654	3743
no. of parameters varied	282	350
GOF	1.99	3.28
R	0.064	0.111
R_w	0.076	0.141
max Δ/σ in final cycle	0.01	1.80

$[Y_4(\mu_3\text{-}OCMe_3)_2(\mu\text{-}OCMe_3)_4(OCMe_3)_4(\mu_4\text{-}O)(\mu\text{-}Cl)_2Li_4(\mu\text{-}OCMe_3)_2]_2$ (3). A crystal measuring 0.32 × 0.18 × 0.22 mm was handled as described above for **1**. Lattice parameters were determined from 15 computer-centered reflections with $3° \le 2\theta \le 21°$. Relevant crystal and data collection parameters for the present study are given in Table III. During the data collection, the intensities of three standard reflections measured every 100 reflections remained constant. The data were corrected for absorption. Systematic absences established the space group as $C2/c$ or Cc. Statistics favored the centrosymmetric $C2/c$ and this choice was fully supported at all stages of the structure solution and refinement. Refinement in Cc was also attempted but was not successful.[34]

Direct methods (MULTAN 80) were used to locate the yttrium atoms and difference Fourier techniques provided the positions of the remaining non-hydrogen atoms except for the lithium atoms. A $Y_4(OCMe_3)_{10}OCl_2^{2-}$ structural unit was readily identified. Location of the lithium countercations was complicated by their low atomic number and

(29) Evans, W. J.; Dominguez, R.; Hanusa, T. P. *Organometallics* **1986**, *5*, 263–270.
(30) Evans, W. J.; Bloom, I.; Hunter, W. E.; Atwood, J. L. *Organometallics* **1983**, *2*, 709–714.
(31) Sams, D. B.; Doedens, R. J. *Inorg. Chem.* **1979**, *18*, 153–156.
(32) All computations were carried out with a local version of the UCLA Crystallographic Computing Package (C. E. Strouse).
(33) MULTAN 80, A System of Computer Programs for the Automatic Solution of Crystal Structures from X-Ray Diffraction Data, by P. Main et al., 1980.
(34) Marsh, R. E. *Acta Crystallogr.* **1986**, *B42*, 193–198.

Table IV. Final Fractional Coordinates for Complex **1**

	x	y	z
Y(01)	0.14700 (10)	0.17830 (11)	0.84370 (6)
O(02)	0.1235 (6)	0.3058 (7)	0.8973 (4)
O(06)	0.0672 (7)	0.1766 (7)	0.7848 (4)
O(07)	0.0770 (9)	0.0497 (8)	0.8900 (5)
C(02)	0.1742 (12)	−0.0667 (13)	0.7975 (8)
C(04)	0.0500 (12)	0.3352 (13)	0.9210 (8)
C(05)	0.0585 (13)	0.4448 (15)	0.9377 (8)
C(06)	−0.0160 (13)	0.3258 (23)	0.8834 (10)
C(07)	0.0376 (15)	0.2713 (17)	0.9702 (9)
C(10)	0.1755 (10)	0.4211 (12)	0.7876 (6)
C(12A)	0.3257 (26)	0.6603 (30)	0.8760 (16)
C(12B)	0.1770 (30)	0.6517 (33)	0.9389 (19)
C(15)	0.3223 (18)	0.4371 (24)	1.0711 (8)
C(17)	0.0102 (12)	0.1786 (17)	0.7432 (8)
C(18)	0.0152 (17)	0.0802 (20)	0.7140 (11)
C(19)	−0.0708 (16)	0.1922 (25)	0.7647 (10)
C(20)	0.0242 (19)	0.2662 (25)	0.7094 (11)
C(21)	0.1105 (14)	−0.0124 (15)	0.9326 (8)
C(22)	0.0469 (18)	−0.0941 (16)	0.9344 (12)
C(23)	−0.0270 (17)	−0.0601 (20)	0.9112 (12)
C(24)	−0.0056 (15)	0.0193 (17)	0.8733 (9)
Y(02)	0.2500	0.3642 (2)	0.91960 (10)
Cl(01)	0.2500	0.1497 (4)	0.9281 (2)
O(01)	0.2500	0.0847 (10)	0.8143 (5)
O(03)	0.2500	0.2865 (9)	0.8293 (5)
O(04)	0.2500	0.5143 (10)	0.9017 (5)
O(05)	0.2500	0.3695 (13)	0.9989 (6)
C(01)	0.2500	−0.0074 (19)	0.7835 (11)
C(03)	0.2500	0.0271 (19)	0.7254 (10)
C(08)	0.2500	0.3533 (17)	0.7851 (8)
C(09)	0.2500	0.2869 (15)	0.7351 (8)
C(11)	0.2500	0.6215 (20)	0.9047 (12)
C(13A)	0.2500	0.6461 (57)	0.9620 (33)
C(13B)	0.2500	0.6563 (46)	0.8494 (27)
C(14)	0.2500	0.3748 (31)	1.0533 (11)
C(16)	0.2500	0.2747 (27)	1.0748 (13)
C(25)	0.2500	−0.3091 (38)	0.6333 (20)
C(26)	0.2500	−0.2944 (47)	0.5791 (27)
C(27)	0.2500	−0.3787 (48)	0.5444 (21)
C(28)	0.2500	−0.4788 (41)	0.5543 (22)
C(29)	0.2500	−0.4988 (38)	0.6091 (22)
C(30)	0.2500	−0.4119 (34)	0.6436 (15)

disorder in the structure. Examination of the Y–Cl distances (see below) and close inspection of one of the final difference maps revealed a lithium atom, Li(1), 2.30 (6) Å from Cl(2). This distance is within bonding range when compared to the Li–(μ-Cl) distances of 2.390 (4)–2.412 (6), 2.39 (4), 2.405, and 2.417 (8) Å found in $(C_5Me_5)_2Yb(\mu\text{-}Cl)_2Li(OEt_2)_2$,[35] $(C_5Me_5)_2Ce(\mu\text{-}Cl)_2Li(OEt_2)_2$,[36] $[(Me_3Si)_2C_5H_3]_2Nd(\mu\text{-}Cl)_2Li(THF)_2$,[37] and $Cr[OC(CMe_3)_3]_2LiCl(THF)_2$,[38] respectively. An additional pair of $OCMe_3$ groups were found near this lithium position with Li–O bond distances of 2.08 (6) Å (Li(1)–O(12)) and 1.95 (6) Å (Li(1)–O(13)).[39] The alkoxide group containing O(12) forms a bridge between Li(1) and its symmetry-related counterpart Li(1′) in the other half of the molecule. This O(12)–Li(1′) distance is 2.20 (6) Å. The angles around O(12), i.e., Li(1)–O(12)–Li(1′), 95.6 (23)°, Li(1)–O(12)–C(40), 123.3 (25)°, and Li(1′)–O(12)–C(40), 117.9 (23)°, average to 112.3°, which is closer to that expected for tetrahedral rather than trigonal coordination around O(12), suggesting that O(12) interacts with another lithium atom. The unusual Li(1)–O(13)–C(44) angle, 131 (3)°, suggested that O(13) was also interacting with a lithium atom. Positions for additional lithium atoms were calculated by using idealized tetrahedral and trigonal-planar geometries around O(12) and O(13), respectively, and were labeled Li(a) and Li(b), respectively. Lithium atoms in these positions would be within bonding distance of Cl(1). The long Y(1)–Cl(1) distance of 2.682 (9) Å is consistent with this sort of bonding interaction for Cl(1).

In addition to this apparent $[Li(OCMe_3)_2Li_2]_2$ bridging unit, there must be two other symmetry-related lithium atoms in the lattice. Although additional electron density has been found on subsequent difference maps, it is spread out too much (i.e., disordered) to define specific lithium positions. All atoms with the exception of the *tert*-butyl carbon atoms and those of the $Li(OCMe_3)_2$ fragment were refined with anisotropic thermal parameters by using full-matrix least-squares methods. Hydrogen atoms were not located. The methyl groups of the *tert*-butyl moieties were disordered, presumably due to rotation about the oxygen–carbon bond. The most intense peaks were labeled as carbon atoms and the residual peaks ignored. Two of the methyl carbon atoms on different *tert*-butoxide groups could not be refined presumably because of this disorder. A final difference map revealed two peaks of intensities 0.53 and 0.42 e Å^{-3}, 1.70 and 1.84 Å away from Cl(1). The peaks were labeled as lithium atoms but did not refine properly and were subsequently deleted. The remaining peaks could be attributed to residual electron density from the heavy metals or *tert*-butoxide ligands, with no other recognizable features. Final fractional coordinates and selected

Table V. Selected Bond Distances for **1** and **3**

1		3	
	Y–O (OR terminal)		
Y(1)–O(6)	2.037 (11)	Y(1)–O(7)	2.03 (2)
Y(2)–O(5)	2.05 (2)	Y(2)–O(8)	2.02 (2)
		Y(3)–O(9)	2.07 (2)
		Y(4)–O(10)	2.03 (2)
	Y–O(μ-OR)		
Y(1)–O(1)	2.285 (9)	Y(1)–O(1)	2.26 (2)
Y(1)–O(2)	2.241 (10)	Y(1)–O(2)	2.34 (2)
Y(2)–O(2)	2.358 (10)	Y(2)–O(3)	2.29 (2)
		Y(2)–O(4)	2.28 (2)
		Y(3)–O(2)	2.28 (2)
		Y(3)–O(3)	2.30 (2)
		Y(4)–O(1)	2.26 (2)
		Y(4)–O(4)	2.28 (2)
	Y–O(μ_3-OR)		
Y(1)–O(3)	2.306 (8)	Y(1)–O(5)	2.41 (2)
Y(2)–O(3)	2.556 (13)	Y(2)–O(6)	2.35 (2)
		Y(3)–O(5)	2.41 (2)
		Y(3)–O(6)	2.36 (2)
		Y(4)–O(5)	2.37 (2)
		Y(4)–O(6)	2.44 (2)
	Y–O(THF) or Y–O(oxide)		
Y(1)–O(7)[a]	2.417 (12)	Y(1)–O(11)[b]	2.52 (2)
		Y(2)–O(11)[b]	2.47 (2)
		Y(3)–O(11)[b]	2.44 (2)
		Y(4)–O(11)[b]	2.40 (2)
	Y–Cl(μ_3-Cl) or Y–Cl(μ-Cl)		
Y(1)–Cl(1)[c]	2.820 (5)	Y(1)–Cl(1)[d]	2.681 (9)
Y(2)–Cl(2)[c]	2.897 (6)	Y(2)–Cl(2)[d]	2.700 (8)

[a] Y–O(THF). [b] Y–O(oxide). [c] Y–Cl(μ_3-Cl). [d] Y–Cl(μ-Cl).

Table VI. Selected Bond Angles for Complex **1**

O(06)–Y(01)–O(02)	110.6 (4)	O(04)–Y(02)–Cl(01)	171.5 (4)
O(06)–Y(01)–O(01)	104.8 (4)	O(02)–Y(02)–O(02)′	131.2 (5)
O(06)–Y(01)–O(03)	113.0 (4)	O(02)–Y(02)–O(03)	68.9 (2)
O(06)–Y(01)–O(07)	92.0 (5)	O(02)–Y(02)–Cl(01)	71.7 (2)
O(06)–Y(01)–Cl(01)	171.0 (3)	O(03)–Y(02)–Cl(01)	70.2 (3)
O(02)–Y(01)–O(01)	139.8 (4)	Y(01)–Cl(01)–Y(01′)	76.6 (2)
O(02)–Y(01)–O(03)	75.6 (4)	Y(01)–Cl(01)–Y(02)	78.77 (15)
O(02)–Y(01)–O(07)	99.0 (4)	C(01)–O(01)–Y(01)	130.1 (3)
O(02)–Y(01)–Cl(01)	74.8 (3)	Y(01)–O(01)–Y(01′)	99.8 (5)
O(01)–Y(01)–O(03)	73.4 (4)	C(04)–O(02)–Y(01)	128.7 (10)
O(01)–Y(01)–O(07)	98.4 (4)	C(04)–O(02)–Y(02)	126.3 (10)
O(01)–Y(01)–Cl(01)	73.0 (3)	Y(01)–O(02)–Y(02)	104.1 (4)
O(03)–Y(01)–O(07)	154.9 (5)	C(08)–O(03)–Y(01)	121.2 (6)
O(03)–Y(01)–Cl(01)	75.0 (3)	C(08)–O(03)–Y(02)	117.6 (11)
O(07)–Y(01)–Cl(01)	79.9 (4)	Y(01)–O(03)–Y(01′)	98.6 (5)
O(05)–Y(02)–O(04)	100.9 (6)	Y(01)–O(03)–Y(02)	96.4 (4)
O(05)–Y(02)–O(02)	104.8 (3)	C(11)–O(04)–Y(02)	164.0 (15)
O(05)–Y(02)–O(03)	157.8 (6)	C(14)–O(05)–Y(02)	179.1 (22)
O(05)–Y(02)–Cl(01)	87.7 (5)	C(17)–O(06)–Y(01)	178.3 (12)
O(04)–Y(02)–O(02)	105.7 (3)	C(21)–O(07)–Y(01)	125.3 (12)
O(04)–Y(02)–O(03)	101.3 (5)	C(24)–O(07)–Y(01)	120.3 (12)

(35) Watson, P. L.; Whitney, J. F.; Harlow, R. L. *Inorg. Chem.* **1981**, *20*, 3271–3278.
(36) Rausch, M. D.; Moriarity, K. J.; Atwood, J. L.; Weeks, J. A.; Hunter, W. E.; Brittain, H. G. *Organometallics* **1986**, *5*, 1281–1283.
(37) Lappert, M. F.; Singh, A.; Atwood, J. L.; Hunter, W. E. *J. Chem. Soc., Chem. Commun.* **1981**, 1190–1191.
(38) Hvoslef, J.; Hope, H.; Murray, B. D.; Power, P. P. *J. Chem. Soc., Chem. Commun.* **1983**, 1438–1439.
(39) Cf. with the following Li–O bond distances: 1.95 Å in LiOMe,[40] 1.830 (12)–2.009 (11) Å in $[LiOC(CMe_3)_3(THF)]_2$,[38] and 1.849 (11)–1.867 (10) Å in $[Li(OC_6H_2Me\text{-}4\text{-}(t\text{-}Bu)_2\text{-}2,6)(OEt_2)]_2$.[41]
(40) Wheatley, P. J. *J. Chem. Soc.* **1960**, 4270–4274.
(41) Cetinkaya, B.; Gumrukcu, I.; Lappert, M. F.; Atwood, J. L.; Shakir, R. *J. Am. Chem. Soc.* **1980**, *102*, 2086–2088.

Table VII. Final Fractional Coordinates for Complex 3

	x	y	z
Y(01)	0.4263 (1)	0.3143 (2)	0.6059 (1)
Y(02)	0.3166 (1)	0.0177 (2)	0.6176 (1)
Y(03)	0.4518 (1)	0.0764 (2)	0.6233 (1)
Y(04)	0.3481 (1)	0.2077 (2)	0.6668 (1)
Cl(01)	0.3696 (4)	0.3247 (7)	0.5521 (2)
Cl(02)	0.2810 (3)	0.0917 (6)	0.5621 (2)
O(01)	0.3543 (7)	0.3455 (14)	0.6386 (4)
O(02)	0.4806 (7)	0.1891 (14)	0.5869 (5)
O(03)	0.3980 (7)	-0.0272 (14)	0.5960 (4)
O(04)	0.2746 (7)	0.1284 (14)	0.6494 (4)
O(05)	0.4412 (7)	0.2221 (12)	0.6538 (4)
O(06)	0.3779 (7)	0.0437 (13)	0.6585 (4)
O(07)	0.4737 (9)	0.4318 (16)	0.6021 (5)
O(08)	0.2703 (7)	-0.1001 (15)	0.6218 (5)
O(09)	0.5190 (8)	0.0044 (16)	0.6392 (5)
O(10)	0.3379 (8)	0.2355 (17)	0.7145 (5)
O(11)	0.3703 (6)	0.1654 (12)	0.6119 (4)
C(01)	0.3247 (14)	0.4269 (29)	0.6409 (9)
C(02)	0.5256 (15)	0.1922 (31)	0.5626 (10)
C(03)	0.4107 (14)	-0.1021 (28)	0.5753 (9)
C(04)	0.2179 (12)	0.1338 (23)	0.6591 (7)
C(05)	0.4811 (12)	0.2655 (25)	0.6742 (8)
C(06)	0.3796 (14)	-0.0290 (29)	0.6844 (9)
C(07)	0.5018 (16)	0.5192 (34)	0.5930 (11)
C(08)	0.2377 (16)	-0.1854 (32)	0.6196 (10)
C(09)	0.5680 (24)	-0.0413 (49)	0.6689 (16)
C(10)	0.3223 (20)	0.2444 (41)	0.7486 (13)
C(11)	0.2757 (16)	0.4231 (31)	0.6135 (10)
C(12)	0.3603 (17)	0.5166 (34)	0.6281 (11)
C(13)	0.3014 (16)	0.4487 (31)	0.6742 (11)
C(14)	0.5109 (20)	0.2601 (40)	0.5350 (13)
C(15)	0.5354 (23)	0.1005 (48)	0.5504 (14)
C(16)	0.4694 (16)	-0.1244 (31)	0.5725 (10)
C(17)	0.3926 (22)	-0.0684 (44)	0.5424 (15)
C(18)	0.3797 (23)	-0.1953 (45)	0.5857 (15)
C(19)	0.2087 (13)	0.2330 (26)	0.6733 (8)
C(20)	0.2039 (14)	0.0588 (29)	0.6824 (9)
C(21)	0.1870 (14)	0.1203 (29)	0.6295 (9)
C(22)	0.5363 (12)	0.2721 (23)	0.6584 (8)
C(23)	0.4624 (15)	0.3632 (31)	0.6861 (9)
C(24)	0.4876 (12)	0.2061 (24)	0.7044 (8)
C(25)	0.4210 (14)	0.0001 (29)	0.7133 (9)
C(26)	0.3198 (14)	-0.0364 (27)	0.7009 (9)
C(27)	0.3989 (14)	-0.1274 (29)	0.6675 (9)
C(28)	0.5658 (17)	0.4853 (33)	0.5866 (11)
C(29)	0.4971 (24)	0.5925 (47)	0.6214 (15)
C(30)	0.4880 (18)	0.5675 (37)	0.5615 (12)
C(31)	0.2609 (19)	-0.2596 (40)	0.6453 (13)
C(32)	0.1826 (23)	-0.1559 (43)	0.6362 (14)
C(33)	0.2376 (20)	-0.2382 (42)	0.5883 (14)
C(34)	0.5939 (29)	-0.0340 (59)	0.6324 (19)
C(36)	0.5625 (25)	-0.1374 (51)	0.6377 (16)
C(37)	0.3614 (23)	0.3219 (44)	0.7562 (14)
C(38)	0.3445 (25)	0.1603 (48)	0.7689 (16)
C(39)	0.2736 (24)	0.2987 (45)	0.7536 (15)
C(40)	0.3421 (14)	0.2032 (28)	0.4668 (9)
C(41)	0.3058 (13)	0.1699 (25)	0.4391 (9)
C(42)	0.3772 (15)	0.2936 (30)	0.4539 (10)
C(43)	0.3765 (14)	0.1146 (29)	0.4796 (9)
C(44)	0.1945 (16)	-0.0572 (32)	0.4949 (11)
C(45)	0.1814 (20)	-0.0954 (39)	0.4583 (13)
C(46)	0.1627 (21)	-0.0649 (41)	0.5286 (14)
C(47)	0.2510 (20)	-0.0942 (34)	0.4994 (12)
O(12)	0.3063 (7)	0.2331 (14)	0.4936 (4)
O(13)	0.2092 (8)	0.0522 (16)	0.4884 (5)
Li(01)	0.2475 (21)	0.1450 (43)	0.5143 (14)

bond length and angle data are given in Tables VII, V, and VIII, respectively, and in the supplementary material.

$Y_3(\mu_3\text{-}OCMe_3)(\mu_3\text{-}Cl)(\mu\text{-}OCMe_3)_3(OCMe_3)_4(THF)_2$ (2) and $La_3(\mu_3\text{-}OCMe_3)_2(\mu\text{-}OCMe_3)_3(OCMe_3)_4(THF)_2$ (4). Preliminary crystallographic studies on **2** and **4** revealed for **2** a hexagonal unit cell with a = 17.648 (11) Å and c = 11.171 (4) Å and for **4** an orthorhombic unit cell with a = 20.543 (11) Å, b = 17.477 (9), and c = 17.905 (7) Å. On the basis of these data, complete crystallographic studies of each were initiated. Although the crystal quality appeared to be good, problems encountered with the structure refinement made the data obtained in both cases unreliable and not sufficiently unambiguous to fully define the structures.

Table VIII. Selected Bond Angles for Complex 3

O(07)-Y(01)-O(01)	109.9 (9)	O(01)-Y(04)-O(11)	73.1 (7)
O(07)-Y(01)-O(02)	104.6 (8)	O(01)-Y(04)-O(06)	135.7 (7)
O(07)-Y(01)-O(05)	113.3 (8)	O(04)-Y(04)-O(05)	139.3 (6)
O(07)-Y(01)-O(11)	177.7 (8)	O(04)-Y(04)-O(11)	75.2 (6)
O(07)-Y(01)-Cl(01)	102.1 (6)	O(04)-Y(04)-O(06)	74.9 (6)
O(01)-Y(01)-O(02)	142.1 (7)	O(05)-Y(04)-O(11)	66.9 (6)
O(01)-Y(01)-O(05)	75.3 (6)	O(05)-Y(04)-O(06)	75.9 (6)
O(01)-Y(01)-O(11)	70.9 (6)	O(11)-Y(04)-O(06)	64.7 (6)
O(01)-Y(01)-Cl(01)	93.6 (5)	O(13)-Li(01)-O(12)	121.0 (29)
O(02)-Y(01)-O(05)	77.0 (6)	O(13)-Li(01)-O(12′)	97.2 (24)
O(02)-Y(01)-O(11)	74.1 (6)	O(13)-Li(01)-Cl(02)	117.0 (28)
O(02)-Y(01)-Cl(01)	94.2 (5)	O(12)-Li(01)-O(12′)	84.4 (23)
O(05)-Y(01)-O(11)	64.7 (6)	O(12)-Li(01)-Cl(02)	106.3 (24)
O(05)-Y(01)-Cl(01)	144.5 (5)	O(12′)-Li(01)-Cl(02)	128.2 (27)
O(11)-Y(01)-Cl(01)	79.9 (5)	Li(01)-Cl(02)-Y(02)	176.0 (14)
O(08)-Y(02)-O(04)	104.8 (8)	C(01)-O(01)-Y(04)	130.6 (20)
O(08)-Y(02)-O(03)	107.9 (7)	C(01)-O(01)-Y(01)	128.6 (20)
O(08)-Y(02)-O(06)	116.5 (8)	Y(04)-O(01)-Y(01)	100.8 (7)
O(08)-Y(02)-O(11)	177.9 (7)	C(02)-O(02)-Y(03)	133.2 (20)
O(08)-Y(02)-Cl(02)	100.8 (6)	C(02)-O(02)-Y(01)	128.7 (21)
O(04)-Y(02)-O(03)	143.7 (7)	C(03)-O(03)-Y(02)	129.5 (18)
O(04)-Y(02)-O(06)	76.8 (6)	C(03)-O(03)-Y(03)	131.1 (19)
O(04)-Y(02)-O(11)	74.0 (6)	Y(02)-O(03)-Y(03)	99.0 (8)
O(04)-Y(02)-Cl(02)	94.4 (5)	C(04)-O(04)-Y(02)	128.4 (17)
O(03)-Y(02)-O(06)	74.8 (6)	C(04)-O(04)-Y(04)	131.9 (16)
O(03)-Y(02)-O(11)	73.8 (6)	Y(02)-O(04)-Y(04)	99.0 (7)
O(03)-Y(02)-Cl(02)	94.6 (5)	C(05)-O(05)-Y(04)	125.5 (16)
O(06)-Y(02)-O(11)	65.0 (6)	C(05)-O(05)-Y(01)	112.3 (16)
O(06)-Y(02)-Cl(02)	142.7 (5)	C(05)-O(05)-Y(03)	126.3 (16)
O(11)-Y(02)-Cl(02)	77.7 (5)	Y(04)-O(05)-Y(01)	93.5 (6)
O(09)-Y(03)-O(02)	107.7 (7)	Y(04)-O(05)-Y(03)	98.0 (7)
O(09)-Y(03)-O(03)	109.7 (8)	Y(01)-O(05)-Y(03)	92.1 (6)
O(09)-Y(03)-O(06)	109.3 (7)	C(06)-O(06)-Y(02)	116.8 (18)
O(09)-Y(03)-O(05)	108.7 (7)	C(06)-O(06)-Y(03)	123.0 (17)
O(09)-Y(03)-O(11)	172.6 (7)	C(06)-O(06)-Y(04)	124.0 (18)
O(02)-Y(03)-O(03)	106.6 (6)	Y(02)-O(06)-Y(03)	95.4 (7)
O(02)-Y(03)-O(06)	140.1 (6)	Y(02)-O(06)-Y(04)	92.7 (6)
O(02)-Y(03)-O(05)	77.9 (7)	Y(03)-O(06)-Y(04)	97.7 (7)
O(02)-Y(03)-O(11)	76.5 (6)	C(07)-O(07)-Y(01)	167.8 (24)
O(03)-Y(03)-O(06)	74.2 (6)	C(08)-O(08)-Y(02)	171.4 (23)
O(03)-Y(03)-O(05)	137.5 (6)	C(09)-O(09)-C(34)	50.5 (25)
O(03)-Y(03)-O(11)	74.1 (6)	C(10)-O(10)-Y(04)	169.9 (26)
O(06)-Y(03)-O(05)	76.5 (6)	Y(04)-O(11)-Y(03)	96.5 (7)
O(06)-Y(03)-O(11)	65.2 (6)	Y(04)-O(11)-Y(02)	90.3 (6)
O(05)-Y(03)-O(11)	65.8 (6)	Y(04)-O(11)-Y(01)	90.1 (6)
O(10)-Y(04)-O(01)	110.3 (8)	Y(03)-O(11)-Y(02)	90.3 (6)
O(10)-Y(04)-O(04)	108.9 (8)	Y(03)-O(11)-Y(01)	88.9 (5)
O(10)-Y(04)-O(05)	107.5 (7)	Y(02)-O(11)-Y(01)	179.1 (8)
O(10)-Y(04)-O(11)	173.0 (7)	C(40)-O(12)-Li(01)	123.3 (25)
O(10)-Y(04)-O(06)	110.4 (8)	C(40)-O(12)-Li(01′)	117.9 (23)
O(01)-Y(04)-O(04)	107.2 (7)	Li(01)-O(12)-Li(01′)	95.6 (23)
O(01)-Y(04)-O(05)	76.0 (6)	C(44)-O(13)-Li(01)	131.2 (28)

Results

$Y_3(\mu_3\text{-}OCMe_3)(\mu_3\text{-}Cl)(\mu\text{-}OCMe_3)_3(OCMe_3)_4(THF)_2$ (1). The reaction of YCl_3 with 3 equiv of $NaOCMe_3$ in THF gives a single primary product in 80% yield. ^1H NMR spectra of samples of **1** in C_6D_6 contain several broad overlapping resonances in the δ 1.1–2.1 region attributable to the alkoxide ligands. In THF-d_8, these resonances split into six sharp well-resolved signals with relative intensities of 1:2:1:2:1:1. The complexity of this spectrum suggested that **1** was not simply $Y(OCMe_3)_3$ and an X-ray crystallographic study was initiated. This revealed that **1** is a trimetallic compound with the formula given in eq 5.

$$YCl_3 + 3NaOCMe_3 \xrightarrow{THF} \underset{\mathbf{1}}{Y_3(OCMe_3)_8Cl(THF)_2} \quad (5)$$

As shown in Figure 1, the three metal atoms in **1** comprise a triangle which has μ-$OCMe_3$ groups bridging each edge. Above the triangle is a μ_3-Cl ligand and below is a μ_3-$OCMe_3$ group. One yttrium atom has two terminal $OCMe_3$ ligands; each of the other two yttrium atoms are ligated by one terminal $OCMe_3$ ligand and a molecule of THF. This overall ligand arrangement results in a six-coordinate environment composed of five oxygen donor atoms and a chloride for each yttrium. Both THF groups are located on the same side of the trimetallic plane as the chloride ligand. The molecule has a mirror plane which contains Y(2), Cl, O(1), C(1), C(3), O(3), C(8), C(9), O(4), C(11), C(13), O(5),

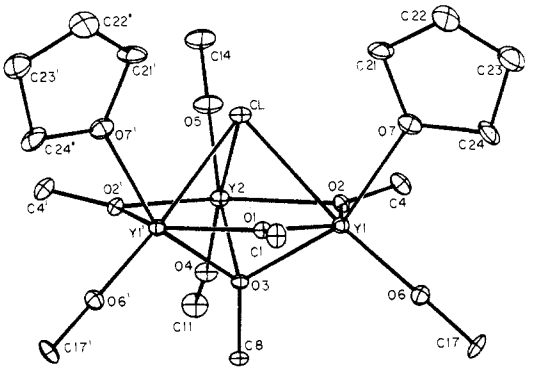

Figure 1. ORTEP drawing of the molecular structure of $Y_3(\mu_3\text{-}OCMe_3)(\mu_3\text{-}Cl)(\mu\text{-}OCMe_3)_3(OCMe_3)_4(THF)_2$ (**1**) with 5% probability ellipsoids. The methyl groups of the *tert*-butoxide ligands have been omitted for clarity.

C(14), and C(16). Disorder was found in the $OCMe_3$ ligand containing O(4) and hence C(12) and C(13) have partial occupancy sites A and B.

The structure of **1** contains eight $OCMe_3$ groups in six distinct environments. This correlates nicely with the 1:2:1:2:1:1 pattern of $OCMe_3$ resonances in the ^1H NMR spectrum of **1**. Furthermore, the shifts of the $OCMe_3$ resonances fall into a pattern in which increased bridging is associated with lower field shifts. Hence, the bridging alkoxide group observed furthest downfield at δ 1.88 may be assigned to the μ_3-$OCMe_3$ group, the δ 1.50 and 1.43 resonances (2:1 ratio) to the μ-$OCMe_3$ groups, and the δ 1.31, 1.24, and 1.22 resonances (2:1:1 ratio) to the three types of terminal $OCMe_3$ groups. This trend in shift versus connectivity is followed in every structurally characterized alkoxide we have studied to date (vide infra). This trend has previously been noted,[18] although not documented by X-ray data. The ^{13}C NMR spectrum of **1** in THF-d_8 shows six chemically inequivalent $OCMe_3$ groups with the quaternary carbon signals in the 76.9–72.1-ppm range and the methyl-carbon resonances in the 36.4–35.2 range. Only five of the six expected methyl resonances were resolved.

Selected bond length and angle data on complex **1** are given in Tables V and VI, respectively. The shortest Y–O distances are 2.037 (11)–2.073 (15) Å and involve terminal $OCMe_3$ groups. As expected,[42] the bridging $OCMe_3$ groups have longer Y–O distances and the average Y–O(μ_3-$OCMe_3$) distance, 2.39 (12) Å, is longer than the average Y–O(μ-$OCMe_3$) length, 2.30 (5) Å. There is some overlap in the ranges of these lengths, however, because the $Y(OCMe_3)_2$ unit (i.e, Y(2)) has longer bridging Y–O (and Y–Cl) distances than the $Y(OCMe_3)(THF)$ parts (i.e., Y(1)) of the trimer. The Y(1)–O(μ-$OCMe_3$) distances of 2.241 (10)–2.285 (9) Å are similar to the 2.19 (2)–2.25 (2) Å lengths observed for Y–O(μ-OMe) distances in $(C_5H_5)_5Y_5(\mu\text{-}OMe)_4(\mu_3\text{-}OMe)_4(\mu_5\text{-}O)$ (**5**)[12] and the doubly bridging Y–O lengths of 2.275 (3) and 2.290 (3) Å in $[(C_5H_5)_2Y(\mu\text{-}OCH{=}CH_2)]_2$ (**6**).[43] This similarity is interesting considering that the yttrium atoms in **5** and **6** are formally eight coordinate (counting C_5H_5 as occupying 3 coordination positions) whereas the yttrium positions in **1** are six coordinate. The Y(1)–O(μ_3-$OCMe_3$) distance of the triply bridging alkoxide group, 2.306 (8) Å, is within the range of Y–O(μ_3-OMe) distances, 2.30 (2)–2.46 (2) Å, found in **5**. The Y(1)–Cl distance of 2.820 (5) Å is longer than any previously characterized Y–Cl bond.[42] This is reasonable, since the Cl is triply bridging in **1** and in all other complexes it is doubly bridging at most. The longest previously reported Y–Cl distance in the literature is 2.776 (5) Å in $(C_5Me_5)_2Y(\mu\text{-}Cl)YCl(C_5Me_5)_2$.

The Y(2) bridging ligand distances are outside the ranges established above. The Y(2)–O(μ-$OCMe_3$) length of 2.358 (10) Å is in the longer μ_3-$OCMe_3$ range and the Y(2)–O(μ_3-$OCMe_3$) distance of 2.556 (13) Å is much longer than the previously observed μ_3-$OCMe_3$ lengths. Y(2)–Cl, 2.897 (6) Å, is also longer than Y(1)–Cl, 2.820 (5) Å. These longer distances may result from steric crowding which prevents the $Y(OCMe_3)_2$ unit from getting in as close to the center of the triangle as the $Y(OCMe_3)(THF)$ groups.

There is other evidence for steric crowding in this molecule. The Y(1)–O(6)–C(17) and Y(2)–O(5)–C(14) angles of 178.3 (12)° and 179.1 (22)° are nearly linear. The Y(2)–O(4)–C(11) angle, on the other hand, is 164.0 (15)° and is bent to move the CMe_3 group away from the center of the molecule. This side of the molecule which contains four $OCMe_3$ groups is more crowded than the other side. The bent Y(2)–O(4)–C(11) unit contains the yttrium atom which is farthest away from the triangle's center. Presumably, both distortions are caused by steric factors. Another aspect of this crowding is that the doubly bridging groups are displaced from the trimetallic plane in the direction of the chloride ligand: 0.031 Å for O(2) and 0.179 Å for O(1).

The Y(1)–O(7) distance of 2.417 (12) Å connecting THF to yttrium is longer than the 2.26 (3)–2.31 (2) Å distances found in $(C_5H_5)_2LnR(THF)$ complexes (Ln = Lu, Yb; R = Me, CMe_3, CH_2SiMe_3)[29,44,45] even after the 0.022–0.032 Å larger size[46] of yttrium is considered. This Y–O distance in **1** is less than the 2.460 (8) Å Y–THF connection in $[(CH_3C_5H_4)_2Y(\mu\text{-}H)(THF)]_2$,[47] however.

$Y_3(\mu_3$-$OCMe_3)(\mu_3$-Cl)(μ-$OCMe_3)_3(OCMe_3)_4(THF)_2$ (2). When YCl_3 reacts with 3 equiv of $NaOCMe_3$ in the presence of *tert*-butyl alcohol a new product, **2**, is obtained. The ^1H NMR spectrum of **2** in aromatic solvents like that of **1** contains broad unresolved resonances in the alkoxide region. Variable-temperature NMR studies on **2** in toluene-d_8 showed that the broad resonances sharpened to the clean six-line pattern at 0 °C. Addition of a drop of THF-d_8 to a sample of **2** in benzene-d_6 also gave a spectrum containing a well-resolved six-line pattern and a similar result was obtained in pure THF-d_8. The spectrum of **2** in THF-d_8 has the same number of lines with the same integration pattern as found for **1**, but the $OCMe_3$ resonances have slightly different chemical shifts. The ^1H NMR spectrum of **2** in pyridine-d_5 established the presence of THF ligands in the complex. The ^{13}C NMR spectrum of **2** in THF-d_8 is also similar to that observed for **1**: quaternary carbons for six $OCMe_3$ groups are observed in the 74.4–71.8-ppm range and five methyl resonances are found in the 36.9–35.7-ppm range. The IR and analytical data on **1** and **2** are essentially identical. Attempts to crystallographically establish the structure of **2** were unsuccessful due to what we suspect are disorder problems.

The similarity of **2** to **1** suggested that they may be isomers. There are two isomers of **1** which vary only in the position of the THF ligands. One has both THF molecules on the μ_3-$OCMe_3$ side of the Y_3 triangle and another has one THF molecule on each side of the Y_3 plane. The former structure would have a ^1H NMR spectral pattern like that of **1**, whereas the latter complex would not. On the basis of these data, we believe that **2** is the isomer of **1** in which both THF groups lie on the μ_3-$OCMe_3$ side of the trimetallic plane. In support of this, the ^1H NMR resonance assigned to the μ_3-$OCMe_3$ group is the most shifted signal in **2** compared to the spectrum of **1**. This resonance shifts 0.77-ppm upfield, whereas the remaining ligand resonances shift by no more than 0.04 ppm. The μ_3-$OCMe_3$ group is the one most affected by the difference in geometry between **1** and **2**.

To further establish that **2** is an isomer of **1**, we have looked for synthesis conditions which generate mixtures of **1** and **2** and we have examined isomerization reactions. We have not observed any of the possible isomers of **1** in the reaction of YCl_3 with $NaOCMe_3$. However, if the reaction of YCl_3 with $NaOCMe_3$

(42) Evans, W. J.; Peterson, T. T.; Rausch, M. D.; Hunter, W. E.; Zhang, H.; Atwood, J. L. *Organometallics* **1985**, *4*, 554–559.
(43) Evans, W. J.; Dominguez, R.; Hanusa, T. P. *Organometallics* **1986**, *5*, 1291–1296.
(44) Evans, W. J.; Wayda, A. L.; Hunter, W. E.; Atwood, J. L. *J. Chem. Soc., Chem. Commun.* **1981**, 292–293.
(45) Schumann, H.; Genthe, W.; Bruncks, N.; Pickardt, J. *Organometallics* **1982**, *1*, 1194–1200.
(46) Cotton, F. A.; Wilkinson, G. *Advanced Inorganic Chemistry*, 4th ed.; Wiley: New York, 1980.
(47) Evans, W. J.; Meadows, J. H.; Wayda, A. L.; Hunter, W. E.; Atwood, J. L. *J. Am. Chem. Soc.* **1982**, *104*, 2008–2014.

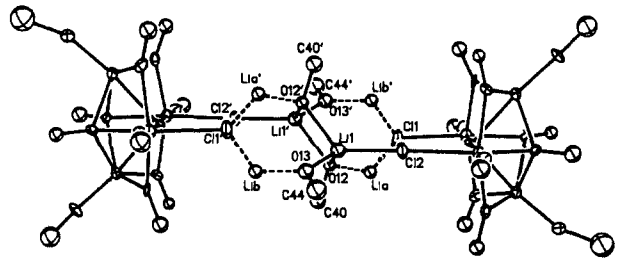

Figure 2. ORTEP drawing of the molecular structure of $[Y_4(\mu_3\text{-}OCMe_3)_2(\mu\text{-}OCMe_3)_4(OCMe_3)_4(\mu_4\text{-}O)(\mu\text{-}Cl)_2Li_4(\mu\text{-}OCMe_3)_2]_2$ (**3**) with 5% probability ellipsoids showing the $[Li(OCMe_3)_2Li_2]_2$ bridging unit and the orientation of the Y_4 units. The methyl groups of the *tert*-butoxide ligands have been omitted for clarity.

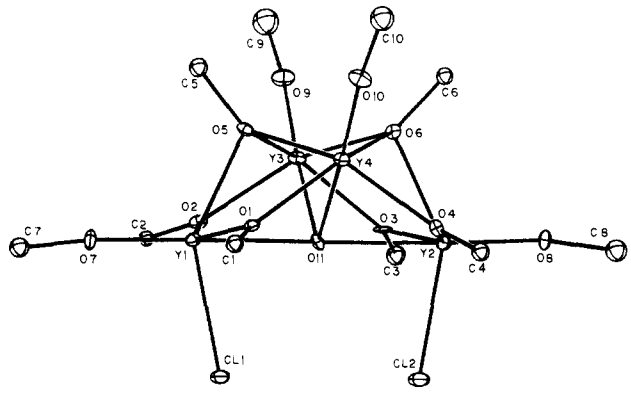

Figure 3. ORTEP drawing of the tetrametallic $Y_4(\mu_3\text{-}OCMe_3)_2(\mu\text{-}OCMe_3)_4(OCMe_3)_4(\mu_4\text{-}O)(\mu\text{-}Cl)_2^{2-}$ portion of **3**. The methyl groups of the *tert*-butoxide ligands have been omitted for clarity.

in the presence of Me_3COH (the synthetic route to **2**) is done at −78 °C for only 1 h, a mixture of **1** and **2** is obtained. Since **2** is the exclusive product at room temperature with longer reaction times, this suggested that any initially formed **1** may be converted to **2**. Indeed, treatment of **1** with Me_3COH, the co-reagent which differentiates the synthesis of **2** from that of **1**, gives **2** by an isomerization process. The reaction is slow at room temperature, but it can be accelerated by heating to 60–80 °C. The clean rearrangement of **1** to **2** coupled with the spectroscopic data strongly supports the assignment of **2** as an isomer of **1**.

$[Y_4(\mu_3\text{-}OCMe_3)_2(\mu\text{-}OCMe_3)_4(OCMe_3)_4(\mu_4\text{-}O)(\mu\text{-}Cl)_2Li_4(\mu\text{-}OCMe_3)_2]_2$ (3). If YCl_3 is reacted with 3 equiv of $LiOCMe_3$ instead of $NaOCMe_3$, this lithium reaction analogous to eq 5 takes a different course. A complex product mixture is obtained which does not contain **1**. Partial separation of this mixture into three different fractions on the basis of solubility in hexane, toluene, and THF was achievable, but no single fully characterizable complex was readily isolated. Varying the stoichiometry in this lithium-containing reaction from 3 equiv of $LiOCMe_3$ per YCl_3 to 2 equiv also gives a mixture of products, but in this case separation by hexane extraction gives a crystalline product, **3**, along with toluene and THF fractions. The ^1H NMR spectrum of the crude product from which **3** was obtained shows multiple $OCMe_3$ resonances. However, once **3** was crystallized, it was no longer soluble, even in THF. Once again X-ray crystallography was necessary for characterization.

For complex **3**, the quality of the data, the complexity of the structure, and the difficulty inherent in structural analysis of disordered and lithium-containing complexes led to a less well defined structure than was obtainable with **1**. Nonetheless, enough reliable structural information was obtained to determine the gross geometry of this species. As shown in Figure 2, complex **3** contains two $Y_4(\mu_3\text{-}OR)_2(\mu\text{-}OR)_4(OR)_4(\mu_4\text{-}O)Cl_2^{2-}$ units (R = CMe_3) which are related by a crystallographic C_2 axis and which are linked by a complex lithium alkoxide bridge. Each of the tetrayttrium units, Figure 3, has a butterfly arrangement of the metals rather than a tetrahedral geometry. As was found in **1** (and **2** and **5**), **3** contains both μ_3-$OCMe_3$ and μ-$OCMe_3$ groups. One triply bridging unit spans Y(1), Y(3), and Y(4) and the other bridges Y(2), Y(3), and Y(4). Each tetrayttrium fragment in **3** contains four μ-$OCMe_3$ groups involving O(1)–O(4).

Given these structural features, each tetrayttrium unit in **3** can be viewed as two $Y_3(\mu_3\text{-}OCMe_3)(\mu_3\text{-}X)(\mu\text{-}OCMe_3)_3$ units (like that of **1**) fused along one edge (Y(3)–Y(4)). The fused edges have lost their μ-$OCMe_3$ groups. The μ_3-X group for each triangle is a mutually shared oxygen atom, O(11), which triply bridges both of the triangles. Since two of the yttrium atoms in each triangle are shared, this results in a μ_4-O unit. Each yttrium atom in **3** also has a terminal $OCMe_3$ group attached to it. For the fusion atoms Y(3) and Y(4) this brings the coordination number to 6 and no additional terminal ligands are present on these atoms. Y(1) and Y(2) on the other hand are also bonded to chloride atoms. With these attachments, these yttrium positions are also six coordinate.

The structural unit described so far, $Y_4(OCMe_3)_{10}OCl_2^{2-}$, is a dianion. The X-ray data provide evidence for a $[Li(OCMe_3)_2Li_2]_2$ bridging unit which holds the two tetrayttrium dianions together, and two other symmetry-related lithium atoms are in the crystal lattice. Since Li(a) and Li(b) were put in at calculated positions, their "bonds" to Cl(1), O(12), and O(13) have been drawn as dotted lines in Figure 3. Although the refinement of all of the lithium positions is not as good as desired, the data do provide useful information on the main feature of interest in **3**, namely the Y–O bonding arrangement.

The Y–O bond lengths in **3** lie within the ranges of values observed for each structural type of $OCMe_3$ ligand in **1** as shown in Table V. A detailed examination of the individual Y–O distances does not reveal any irregular features about specific yttrium positions. The μ_4-O group is located centrally in the molecule with an Y(1)–O–Y(2) angle of 179.1 (8)° and an Y(3)–O–Y(4) angle of 96.5 (7)°. This oxygen atom is slightly closer to Y(3) and Y(4) (Y–O average 2.42 (2) Å) than to Y(1) and Y(2) (Y–O average 2.50 (2) Å). The Cl–Y bond distances of 2.682 (9) and 2.701 (8) Å are consistent with doubly bridging chloride ligands[42,48] as shown in Figure 2.

The Y–O–C angles of the terminal $OCMe_3$ groups in **3** range from 157.1 (23) to 171.4 (23)° with an average of 166 (2)°. As discussed for **1**, these angles tend to be nearly linear except when steric crowding is a factor. As in **1**, the greatest bending in **3** occurs with the terminal $OCMe_3$ groups on the same side of the Y_3 triangle as the μ_3-$OCMe_3$ ligand. The Y–O(6)–C(6) and Y–O(5)–C(5) angles of the triply bridging $OCMe_3$ ligands suggest that the most steric crowding occurs around Y(3) and Y(4). The Y(1)–O(5)–C(5) and Y(2)–O(6)–C(6) angles of 112.3 (16) and 116.8 (18)° are smaller than the analogous Y–O–C angles involving Y(3) and Y(4) which range from 123.0 (17) to 126.3 (16)°. Hence, the μ_3-$OCMe_3$ groups bend away from the Y(3)–Y(4) area of the molecule.

$La_3(\mu_3\text{-}OCMe_3)_2(\mu\text{-}OCMe_3)_3(OCMe_3)_4(THF)_2$ (4). The reaction of $LaCl_3$ with 3 equiv of $NaOCMe_3$, i.e., the lanthanum analogue of eq 5, was also examined. Like the yttrium system, this reaction, eq 6, gives a single primary product in high yield, 87%. The NMR spectral characteristics are like those of **1** and

$$LaCl_3 + 3\ NaOCMe_3 \rightarrow \underset{\mathbf{4}}{La_3(OCMe_3)_9(THF)_2} \qquad (6)$$

2. In aromatic solvents, the ^1H NMR spectrum contains broad resonances characteristic of fluxional behavior. In THF-d_8, the $OCMe_3$ resonances sharpen. Using the structure–shift correlations developed for **1**, **4** contains two equivalent μ_3-$OCMe_3$ groups, three μ-$OCMe_3$ groups in a ratio of 1:2, and four terminal $OCMe_3$ groups. Even at 500 MHz, the terminal $OCMe_3$ signals are not fully resolved, hence the number of distinct environments is uncertain. The high-field ^{13}C NMR spectrum of **4** shows four types of carbon atoms in the 72–77-ppm range observed for the quaternary alkoxide carbon atoms of **1**. This is consistent with the ^1H NMR data. The ^1H and ^{13}C NMR spectra of **4** in pyridine-d_5 also show four resolvable types of alkoxide groups and establish

(48) Evans, W. J.; Grate, J. W.; Levan, K. R.; Bloom, I.; Peterson, T. T.; Doedens, R. J.; Zhang, H.; Atwood, J. L. *Inorg. Chem.* **1986**, *75*, 3614–3619.

the presence of THF ligands. The IR spectrum of **4** was virtually identical with that of **1** and **2**.

Attempts to crystallographically characterize **4** were again complicated by disorder problems. The spectroscopic and analytical data suggest a structure similar to that of **1** and **2**. The structure of **4** is likely to be the same as those of **1** and **2** except that both μ_3-ligands are $OCMe_3$ groups and that one THF ligand is on each side of the La_3 triangle resulting in C_2 symmetry. This structure agrees with the NMR data and places the terminal $OCMe_3$ groups in very similar environments. This may explain why it is difficult to resolve the terminal $OCMe_3$ NMR signals in this case.

Discussion

Structural Features. The compound $Y_3(OCMe_3)_8Cl(THF)_2$ (**1**) is the first crystallographically characterized yttrium alkyloxide complex.[21] It is remarkably more complex than the simple $Y(OCMe_3)_3$ formula expected for the metathesis reaction of YCl_3 with 3 equiv of an alkali metal alkoxide. The isolation of an isomeric complex **2** and the even more complex tetrametallic $Y_4(OCMe_3)_{10}Cl_2O^{2-}$ unit in **3** suggest that this level of complexity may be the rule rather than the exception for yttrium alkoxide complexes with ligands the size of $OCMe_3$.

Although complexes **1–4** are structurally complex, they display some common features. Particularly striking is the prevalence of a triangular unit of three metals connected with three bridging alkoxides and capped on either side by triply bridging ligands. This basic $Ln_3(\mu_3\text{-}OR)(\mu_3\text{-}X)(\mu\text{-}OR)_3$ unit is identical in complexes **1**, **2**, and **4** which differ only in the positions of the terminal ligands, the specific μ_3-ligand involved, and the particular metal, La or Y.

Each tetrayttrium unit in **3** can be considered as an edge fusion of two triangular units of this type. In **3**, the two triangles share one μ_3-ligand which therefore becomes a μ_4-ligand. The other structural modification which occurs is that the edge bridging μ-$OCMe_3$ ligands are no longer present where the edges of two triangles have been fused, The similarity in geometry and bond distance and angle data between **1** and **3** is consistent with the view that **3** is a fused derivative of a system like **1**.

Several molecular structures found in the literature are relevant to the structures of **1–4** and allow us to make even more generalizations on the prevalence of these trimetallic alkoxide units as building blocks. The yttrium complexes most closely related to **1** structurally are the trimetallic cyclopentadienyl species $\{[(C_5H_5)_2Y(\mu\text{-}H)]_3(\mu_3\text{-}H)\}^-$ (**6**),[10] $\{[(C_5H_5)_2Y(\mu\text{-}OMe)]_3(\mu_3\text{-}H)\}^-$ (**7**),[11] and their mixed ligand derivatives $\{[(C_5H_5)_2Y(\mu\text{-}H)]_x[(C_5H_5)_2Y(\mu\text{-}OMe)]_{3-x}(\mu_3\text{-}H)\}^-$ (x = 1, 2) (**8**).[11] Like **1**, complexes **6–8** each have a triangular arrangement of three L_2Y units (where L is a terminal ligand) connected by doubly bridging anionic ligands. Compounds **6–8** also have μ_3-ligands as in **1**, but in **6–8** there is only one μ_3-ligand per three yttrium atoms, a μ_3-hydride located in the plane of the metals. The similarity between **6–8** and **1** can be emphasized by writing the formula of **1** in a parallel fashion as $\{[(Me_3CO)_2Y(\mu\text{-}OCMe_3)][(Me_3CO)(THF)Y(\mu\text{-}OCMe_3)]_2(\mu_3\text{-}OCMe_3)(\mu_3\text{-}Cl)\}$. Comparison of this formula with those of **6–8** clearly shows that replacement of C_5H_5 groups with alkoxides has been successfully achieved as originally desired.

Two more complexes that are structurally related to **1–4** are the pentametallic yttrium complex $(C_5H_5)_5Y_5(\mu\text{-}OMe)_4(\mu_3\text{-}OMe)_4(\mu_5\text{-}O)$ (**5**)[12] and the hexametallic neodymium complex $Nd_6(OCHMe_2)_{17}Cl$ (**9**).[19] The Nd complex, when reported in 1978, was structurally unusual and attested to the complexity possible in lanthanide alkoxide chemistry. In light of the data on **1–4**, however, this structure is not just a structural oddity, As shown schematically in Figure 4 and with the more explicit formula $\{[(RO)Nd(\mu\text{-}OR)]_3(\mu_3\text{-}OR)\}_2(\mu\text{-}OR)_3(\mu_6\text{-}Cl)$ (R = Me_2CH), this structure is composed of two of the basic triangular units that are found in **1**, **2**, and **3** bridged by three μ-OR units and one μ_6-halide. Complex **9** can be regarded as two $[(RO)_2Nd(\mu\text{-}OR)]_3(\mu_3\text{-}OR)(\mu_3\text{-}Cl)$ units connected by sharing the μ_3-Cl position (which becomes a μ_6-Cl) and three terminal

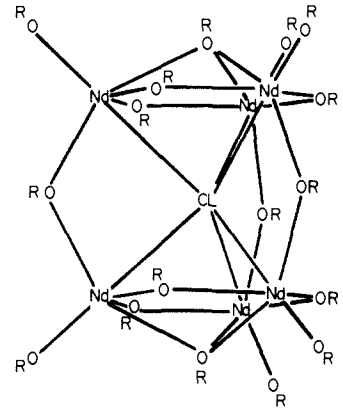

Figure 4. The structure of $[Nd_3(\mu_3\text{-}OR)(\mu\text{-}OR)_3(OR)_3]_2(\mu\text{-}OR)_3(\mu_6\text{-}Cl)$ (**9**) (R = $CHMe_2$).

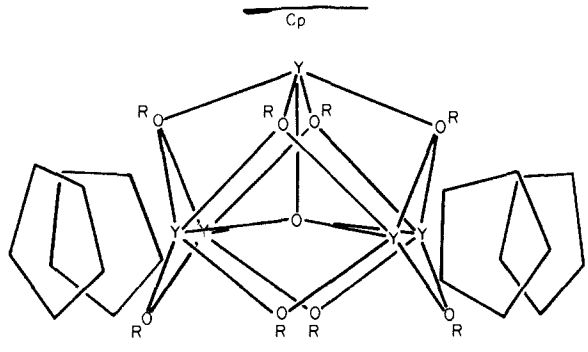

Figure 5. Structure of $(C_5H_5)_5Y_5(\mu_3\text{-}OMe)_4(\mu\text{-}OMe)_4(\mu_5\text{-}O)$ (**5**).

OR groups (which become μ-OR groups). Hence, rather than being an isolated case of an unusually complicated struture, **9** represents another variation on how the basic $Ln_3(\mu_3\text{-}OR)(\mu_3\text{-}X)(\mu\text{-}OR)_3$ units can be assembled.

Complex **5**, shown in Figure 5, constitutes yet another example of an assembly of these triangular units. In **5**, four $Y_3(\mu_3\text{-}OR)(\mu_3\text{-}X)(\mu\text{-}OR)_3$ units have been fused together. In this case the terminal ligands are not alkoxide groups or RO and THF as in **1**. Instead, there is one terminal C_5H_5 group per yttrium atom. As in **3**, fusion of two triangles along an edge eliminates the μ-OR groups. Hence **5** contains only four μ-OR groups around the base of the square pyramid, since each triangle is fused on the two other sides. The four μ_3-OR groups of the original unit are retained in **5** and the four μ_3-X groups are represented by a single centrally shared oxygen atom.

If one considers the polymetallic alkoxide complexes **1–5** and **7–9** as a group, a pattern is evident; the $Ln_3(\mu_3\text{-}OR)(\mu_3\text{-}X)(\mu\text{-}OR)_3$ unit is a basic building block that can generate a variety of structures in yttrium and, in general, lanthanide alkoxide complexes. This unit is stable on its own and can exist in trimetallic complexes. It can also be combined to form larger aggregates, i.e., tetra-, penta-, and hexametallic systems, by fusing edges and/or sharing μ_3-ligands. Considerable variation is possible with the constituents of these trimetallic units. Terminal ligands can be RO, THF, or C_5H_5. The μ_3 and μ_x ($x > 3$) ligands can be H, OR, Cl, or O. Considerable variation in how the triangular units can be assembled is also likely.

The number of possible structural permutations and combinations of the trimetallic units is large. Indeed, the variability in synthetic results discussed in the introduction may be the result of many different structural results. To the extent that molecules of this type can be used as models for heterogeneous metal oxide catalysts and catalyst supports,[49] this structural diversity should provide a wealth of variations with which to precisely model these

(49) See, for example: (a) Rosynek, M. P. *Catal. Rev.-Sci. Eng.* **1977**, *16*, 111–154. (b) Minachev, Kh. M.; Khodakov, Yu. S.; Nakhshunov, V. S. *Russ. Chem. Rev.* **1976**, *45*, 142–154. (c) Sudhaker, C.; Vannice, M. A. *J. Catal.* **1985**, *95*, 227–243. (d) Rieck, J. S.; Bell, A. T. *Ibid.* **1985**, *96*, 88–105.

systems. On the other hand, this could be an impossibly complex synthetic and structural problem. Given the high yields obtainable for **1**, **2**, **4**, and **9** and the NMR correlations demonstrated for **1**, **2**, **4**, and **5**, these systems appear to be manageable.

This structural discussion would not be complete without mentioning some examples of structurally characterized trimetallic alkoxide complexes involving metals other than yttrium and the lanthanides. Such systems have been known for some time. $U_3(OCMe_3)_{10}O$[50] and $Mo_3[(OCH_2(CMe_3)]_{10}O$[51] are two good examples of molecules structurally similar to **1**, **2**, and **4**. Both complexes have the stoichiometry $M_3(\mu_3\text{-}OR)(\mu_3\text{-}O)(\mu\text{-}OR)_3(OR)_6$. They differ in that the uranium and molybdenum are tetravalent not trivalent and, for the molybdenum complex, metal–metal bonds are present. $W_4(OEt)_{16}$,[52] i.e., $[(EtO)_3W(\mu\text{-}OEt)]_2[(EtO)_2W(\mu\text{-}OEt)]_2(\mu_3\text{-}OEt)_2$, and $Mo_4Br_4(OCHMe_2)_8$,[53] i.e., $[(RO)BrMo(\mu\text{-}OR)]_2[BrMo(\mu\text{-}OR)]_2(\mu_3\text{-}OR)_2$ (R = $CHMe_2$), are examples of tetrametallic alkoxide complexes formed by joining two triangular units. The latter molecule has a butterfly geometry like **3**. These examples again differ from the yttrium alkoxide complexes in that metal–metal bonds are present. The above discussion is hardly comprehensive,[54] but it makes the point that structural similarity exists between **1**–**5** and **7**–**9** and polymetallic alkoxides of other metals. It is possible that alkoxide groups will be excellent ligands which allow more direct comparisons of yttrium and the lanthanides with other metals in the periodic table.

There is also a structural similarity between the yttrium alkoxide complexes described here and the recently reported tetravalent zirconium thiolates, $[(Me_3CS)_2Zr(\mu\text{-}SCMe_3)]_3(\mu_3\text{-}SCMe_3)(\mu_3\text{-}S)$[55] and $\{[(BH_4)_2Zr(\mu\text{-}SCMe_3)][(BH_4)(THF)Zr(\mu\text{-}SCMe_3)][(BH_4)(THF)Zr(\mu\text{-}S)](\mu_3\text{-}S)_2\}$.[56] It is likely that thiolate analogues of the yttrium and lanthanide alkoxide complexes will also be accessible.

Synthetic Aspects. Just as remarkable as the structural features of **1**–**4** is the fact that simple ionic metathesis reactions between YCl_3 or $LaCl_3$ and alkali metal alkoxides can assemble compounds (in high yields) as complex as were found. Too little is known at present regarding intermediates and interconversions to comment in detail on how the polymetallic alkoxides are constructed, but some discussion is appropriate at this stage in the development of this area.

Clearly, the details of the syntheses, i.e., the choice of alkali metal countercation, the absence or presence of alcohol during the reaction, and the specific metal used, substantially influence the outcome of the reaction. The importance of minor changes in reaction conditions were also noted in the synthesis of **5**.[12] Given the importance of such details, it is inappropriate to write simple generic synthetic equations such as eq 3 to describe reactions of alkali metal alkoxides with yttrium and lanthanide halides. The variations in products previously reported in the literature[13-27] are likely to result from small differences in how these reactions were conducted. Close attention to synthetic detail is certainly required for any future studies in this area. Some specific synthetic aspects are discussed in the following sections.

Presence of the Cl Ligand in 1 and 2. Attempts to react the μ_3-Cl ligand in **1** and **2** with $NaOCMe_3$ and reactions of YCl_3 with greater than 3 equiv of $NaOCMe_3$ have given predominantly insoluble products. This suggests that the presence of the chloride ligand in **1** and **2** may be critical to the isolation of *soluble* polymetallic products in the yttrium *tert*-butoxide system. Initially,

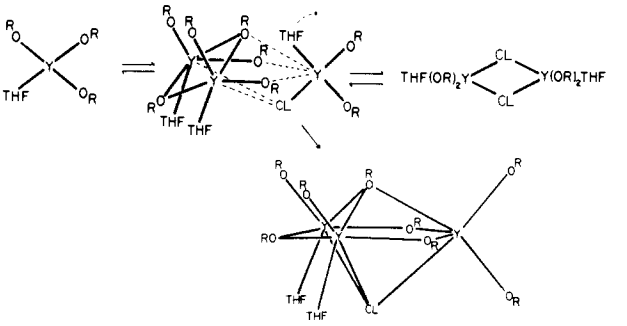

Figure 6. One possible route to complex **1** (R = *tert*-butyl).

a mixture of monometallic species such as $YCl_2(OR)(THF)_x$, $YCl(OR)_2(THF)_x$, and $Y(OR)_3(THF)_x$ may be present in the $YCl_3/NaOCMe_3$ reaction mixture along with the NaCl byproduct. Given the large size of yttrium, its preference for high coordination numbers, and the tendency of complexes of these metals to undergo ligand exchange reactions, it is likely that these monometallic species are in equilibrium with dimeric species of the type $[(THF)_x(RO)_2Y(\mu\text{-}Cl)]_2$, $[(THF)_x(RO)_2Y(\mu\text{-}OR)]_2$, $[(THF)_x(RO)_2Y]_2(\mu\text{-}Cl)(\mu\text{-}OR)$, etc. There are several ways in which a bimetallic species and a monometallic species could combine to form **1**. One example is shown in Figure 6. This hypothetical scheme has a direct parallel in the route likely in the formation of the trimetallic $\{[(C_5H_5)_2Y(\mu\text{-}H)]_3(\mu\text{-}H)\}^-$ complex from bimetallic $[(C_5H_5)_2Y(\mu\text{-}H)(THF)]_2$ complexes.[10]

It is possible that once the multiple equilibria reach the trimetallic μ_3-Cl or μ_3-OR bridged stage, this unit is sufficiently stable that it does not dissociate further and ceases to participate in the active equilibria. Consistent with this, **1** and **2** are not flexible enough to isomerize in solution without the addition of an external reagent.

It is interesting to note that the formation of **1** occurs in a stereospecific manner such that none of isomer **2** is formed. This selectivity may derive from steric factors. Condensation of a dimer with a monomer as shown in Figure 6 may be favorable only when the μ_3-group with the larger donor atom radius, i.e., μ_3-Cl, is oriented to form a trimer in which it is adjacent to the two terminal THF positions, i.e., when it is on the less sterically crowded side. Intermediates leading to a condensation in which μ_3-Cl is on the same side as three terminal OR groups may be sterically disfavored.

Once the $Y_3(\mu_3\text{-}OCMe_3)(\mu_3\text{-}Cl)(\mu\text{-}OCMe_3)_3(OCMe_3)_4(THF)_2$ unit of **1** formed, however, the μ_3-Cl side may actually be the less crowded since the μ_3-Cl ligand comprises a single atom. The larger Me_3C group on the μ_3-$OCMe_3$ ligand may cause considerable crowding on the side containing three terminal $OCMe_3$ groups in the assembled complex. The out-of-plane bending of the μ-$OCMe_3$ groups away from the μ_3-$OCMe_3$ ligand, the nonsymmetrical location of the μ_3-$OCMe_3$ ligand with respect to the three metals, and the bending of the adjacent Y–O–C angle indicate that steric crowding does exist on this side of the triangle in **1**. Hence, although **1** is the kinetically obtained product it may be less stable thermodynamically and as a result it isomerizes to **2**. How the **1**–**2** isomerization is effected by *tert*-butyl alcohol remains to be determined.

La vs Y in 1 vs 4. Complexes **1** and **4** differ in that **4** contains two μ_3-$OCMe_3$ groups and no halide ligand. On the basis of the discussion above, it is likely that an yttrium analogue of **4**, i.e., $Y_3(\mu_3\text{-}OCMe_3)_2(\mu\text{-}OCMe_3)_3(OCMe_3)_4(THF)_2$, would be too sterically crowded. Since La^{3+} is 0.181 Å larger than Y^{3+},[46] the lanthanum system can sterically accommodate two μ_3-$OCMe_3$ groups. Hence, the incorporation of chloride is less synthetically crucial to the formation of soluble *tert*-butoxide complexes of this early lanthanide. This is not to say that chloro alkoxides of the early lanthanides will not form under the proper conditions. An example is $Nd_6(OCHMe_2)_{17}Cl$.[19]

Presence of the Oxide Ligand in 3. At present, the source of the oxide ligand in **3** has not been determined. This is not the first time that an oxide ligand has been found in an yttrium

(50) Cotton, F. A.; Marler, D. O.; Schwotzer, W. *Inorg. Chem. Acta* **1984**, *95*, 207–209.
(51) Chisholm, M. H.; Folting, K.; Huffman, J. C.; Kirkpatrick, C. C. *J. Am. Chem. Soc.* **1981**, *103*, 5967–5968.
(52) Chisholm, M. H.; Huffman, J. C.; Kirkpatrick, C. C.; Leonelli, J.; Folting, K. *J. Am. Chem. Soc.* **1981**, *103*, 6093–6099.
(53) Chisholm, M. H.; Errington, R. J.; Folting, K.; Huffman, J. C. *J. Am. Chem. Soc.* **1982**, *104*, 2025–2027.
(54) See, for example: Chisholm, M. H. *Polyhedron* **1983**, *2*, 681–721.
(55) Coucouvanis, D.; Hadjikyriacou, A.; Kanatzidis, M. G. *J. Chem. Soc., Chem. Commun.* **1985**, 1224–1225.
(56) Coucouvanis, D.; Lester, R. K.; Kanatzidis, M. G.; Kessissoglou, D. P. *J. Am. Chem. Soc.* **1985**, *107*, 8279–8280.

alkoxide reaction. The reaction of $(C_5H_5)_2YCl(THF)$ with KOMe·MeOH also generates an oxide in the product, $(C_5H_5)_5Y_5(\mu\text{-OMe})_4(\mu_3\text{-OMe})_4O$,[12] and we currently are investigating other examples of this phenomena which we have observed.

Li vs Na Countercations. There are numerous examples in organoyttrium and organolanthanide chemistry in which the presence and specific nature of the cation strongly influences the chemistry.[2,57,58] Hence, it is not unreasonable to see different results in the $NaOCMe_3$ vs $LiOCMe_3$ reactions. Given the complexity of the $LiOCMe_3$ reactions compared to the $NaOCMe_3$ systems and the presence of several lithium atoms in **3**, it appears the lithium is more readily carried along in these systems. This leads to a wider variety of products and crystallographically more difficult systems.

Conclusions

The reactions of YCl_3 and $LaCl_3$ with alkali metal alkoxides have provided a new and important class of polylanthanide and polyyttrium alkoxide and oxide complexes. Despite the structural complexity of these complexes it has proven possible to correlate X-ray and ^1H NMR data to allow this chemistry to be followed and monitored by NMR spectroscopy. When several of these complexes are viewed together structural correlations become evident. Most important is the existence of $Ln_3(\mu_3\text{-OR})(\mu_3\text{-X})(\mu\text{-OR})_3$ building blocks from which a variety of structures can be constructed. Since our study used metals representative of both the early (La) and late (Y) lanthanides, this chemistry is likely to be general in the series. These alkoxide complexes have demonstrated that the $OCMe_3$ ligand can be used as a viable replacement for C_5H_5 groups. Given the importance of C_5H_5 as a co-ligand in mono- and bimetallic lanthanide and yttrium organometallic chemistry, it is likely that the $OCMe_3$ ligand will find a similarly important place in the tri- and polymetallic chemistry of these metals. Continued efforts in this area will concentrate on preparing alkyl and hydride derivatives of these and related species.

Acknowledgment. We thank the Division of Chemical Sciences of the Office of Basic Energy Sciences of the Department of Energy for support of the research and Professor R. J. Doedens for his help and advice with the crystal structure determinations.

Registry No. **1**, 112596-07-3; **2**, 112710-05-1; **3**, 112596-10-8; **4**, 112596-08-4.

Supplementary Material Available: A fully-numbered ORTEP plot of **1** plus tables of complete bond distances and angles and thermal parameters (9 pages); listings of observed and calculated structure factors for **1** and **3** (25 pages). Ordering information is given on any current masthead page.

(57) Tilley, T. D.; Andersen, R. A.; Spencer, B.; Ruben, H.; Zalkin, A.; Templeton, D. H. *Inorg. Chem.* **1980**, *19*, 2999-3003.
(58) References 9 and 35. Schumann, H.; Genthe, W. *J. Organomet. Chem.* **1981**, *213*, C7-C9. Schumann, H.; Genthe, W.; Hahn, E.; Hossain, M. B.; van der Helm, D. *J. Organomet. Chem.* **1986**, *299*, 67-84.

Angle Dependence of the Properties of the $[Fe_2X]^{4+}$ Bridge Unit (X = O, S): Structures, Antiferromagnetic Coupling, and Properties in Solution

R. N. Mukherjee, T. D. P. Stack, and R. H. Holm*

Contribution from the Department of Chemistry, Harvard University, Cambridge, Massachusetts 02138. *Received June 26, 1987*

Abstract: The effects of changing the bridge angle θ in the bridges Fe(III)-X-Fe(III) (X = O, S) as they occur in complexes of the type $[Fe(salen)]_2X$ (salen = 1,2-bis(salicylideneaminato)ethane(2-)) have been investigated. The method employed involves escalating steric repulsions between half-dimers by introduction of *t*-Bu groups at ring 3-positions and four methyl groups on the ethylene bridge, affording the complexes $[Fe(3\text{-}t\text{Busaltmen})]_2X$ (X = O (**6**), S (**7**)). Complex **6** (**7**) crystallizes in monoclinic space group $P2_1/a$ with a = 20.395 (3) Å, b = 11.864 (3) Å, c = 24.311 (4) Å, β = 114.61 (1)° (a = 20.931 (8) Å, b = 11.884 (6) Å, c = 24.229 (7) Å, β = 114.34 (2)°), and Z = 4. On the basis of 4417 (3642) unique data with $F_o^2 > 2.5\ \sigma(F_o^2)$, the structures were refined to R = 5.8 (6.5)%. Bridge angles of 173.4 (2)° (**6**) and 167.0 (2)° (**7**) are markedly larger than those of $[Fe(salen)]_2O$ (**8**, 145°) and $[Fe(salen)]_2S$ (**9**, 122°) determined earlier; these complexes have much weaker steric interactions between half-dimers. A scheme for defining the configurations of these molecules in terms of θ and conformational angles $[\Omega_1,\Omega_2]$ is introduced. Antiferromagnetic coupling shows a small but definite increase as θ increases: J = −183 (**8**) and −200 (**6**) cm^{-1} and J = −178 (**9**) and −218 (**7**) cm^{-1}. Bridge Fe-O distances in **6** and **8** are indistinguishable, and thus are not a factor in regulating coupling. J values for **6** and **7** provide the best current evidence that at nearly constant θ values, antiferromagnetic coupling is transmitted more effectively by a sulfido than an oxo bridge. Analysis of magnetic data in solution and determination of hyperfine coupling constants from contact shifts indicates that **6** and **8** retain their solid-state structures in solution and that the larger shifts of **9** versus **8** arise mainly from susceptibility differences, which are primarily controlled by bridge angle. Molecular configurations of **6**-**9** as well as those of recently reported $[Fe(acen)]_2X$ (X = O, S; acen = *N*,*N*'-ethylenebis(acetylacetone iminato(2-)) are predicted within small limits of angular parameters by a van der Waals potential function for intramolecular interactions. Calculations at the extended Hückel level indicate a small preference for a linear and bent bridge (θ = 135-140°) for X = O and S, respectively, at the crystallographically determined conformational angles. Non-bonded repulsions evidently override the linear oxo bridge preference and reinforce the bent sulfido bridge preference. The increase in J values with increasing θ can be rationalized in terms of a MO model of antiferromagnetic coupling with an important π-super-exchange pathway.

A fundamental structural component of the chemistry of Fe(III) is the μ-oxo bridge unit Fe-O-Fe,[1] which is known to occur with variable bridge angles in the range 139-180° but always with antiferromagnetically coupled Fe atoms. The bridge is usually found in the unsupported condition, i.e., in the absence of other bridges. $[Fe(salen)]_2O$ and related compounds (salen = 1,2-bis(salicylideneamino)ethane) are familiar examples of unsupported bridges. This bridge unit also arises in the supported mode.

(1) Murray, K. S. *Coord. Chem. Rev.* **1974**, *12*, 1.

0002-7863/88/1510-1850$01.50/0